Supporting Information

Recovering Lead and Sulfur from Spent Lead Paste by Molten Salt Electrolysis: A Clean and Sustainable Lead and Sulfur Loop

Hongya Wang[1,2], Fengyin Zhou[1], Bingbing Wang[2], Muya Cai[1], Jingjing Zhao[1], Xinyu Li[1], Yongxin Wu[1,2], Xiaowei Liu[2], Xiang Chen[1], Dihua Wang[1,2,3], Huayi Yin[1,2,3]*

1. School of Resource and Environmental Science, Wuhan University, 299 Bayi Road, Wuchang District, Wuhan 430072, P. R. China.
2. Joint Center of Green Manufacturing of Energy Storage Materials of Wuhan University and Chilwee, Wuhan 430072, P. R. China
3. Hubei International Scientific and Technological Cooperation Base of Sustainable Resource and Energy, Wuhan University, Wuhan 430072, P. R. China

*-Corresponding author. Email: yinhuayi@whu.edu.cn (Huayi Yin)

This PDF file includes:

Supporting Information **Fig. S1** to **Fig. S19**;

Tab. S1, **Tab. S2**;

Calculation of energy consumption for this process;

Calculation of SO_2 emissions;

30 pages in total.

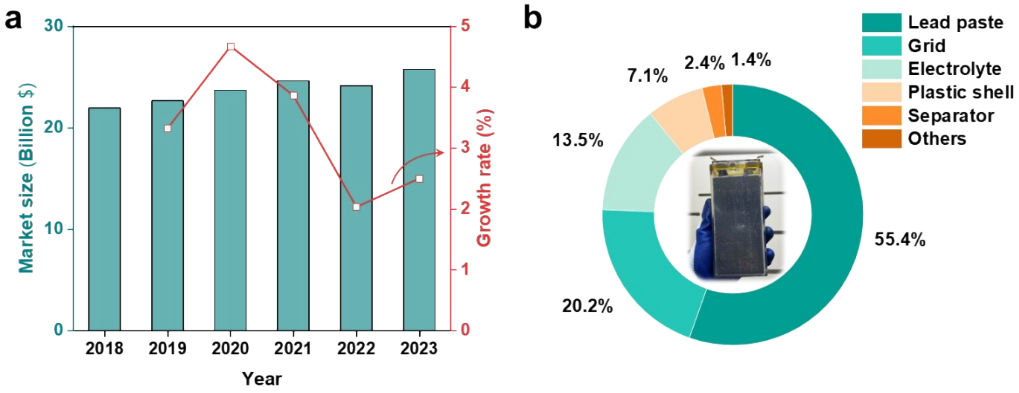

Fig. S1. (a) Global lead-acid battery (LAB) market size and growth rate in recent years, (b) the weight ratio of each component in LAB.

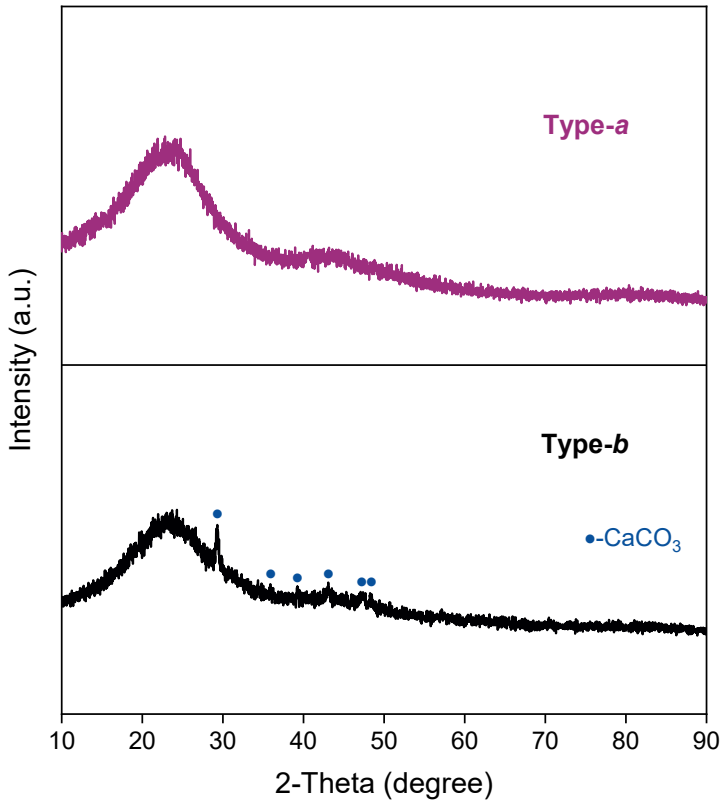

Fig. S2. XRD patterns of charcoal for roasting.

The charcoal used throughout the experimental phase consisted of two types: (***a***) crushed, sieved (≤ 0.1 mm), and then hydrochloric acid (1 M) washed charcoal; and (***b***) crushed, sieved, and used directly (Fig. S2). Type-*b* was applied only to the recovery of 50 g-scale SLP, and the rest were used type-*a*.

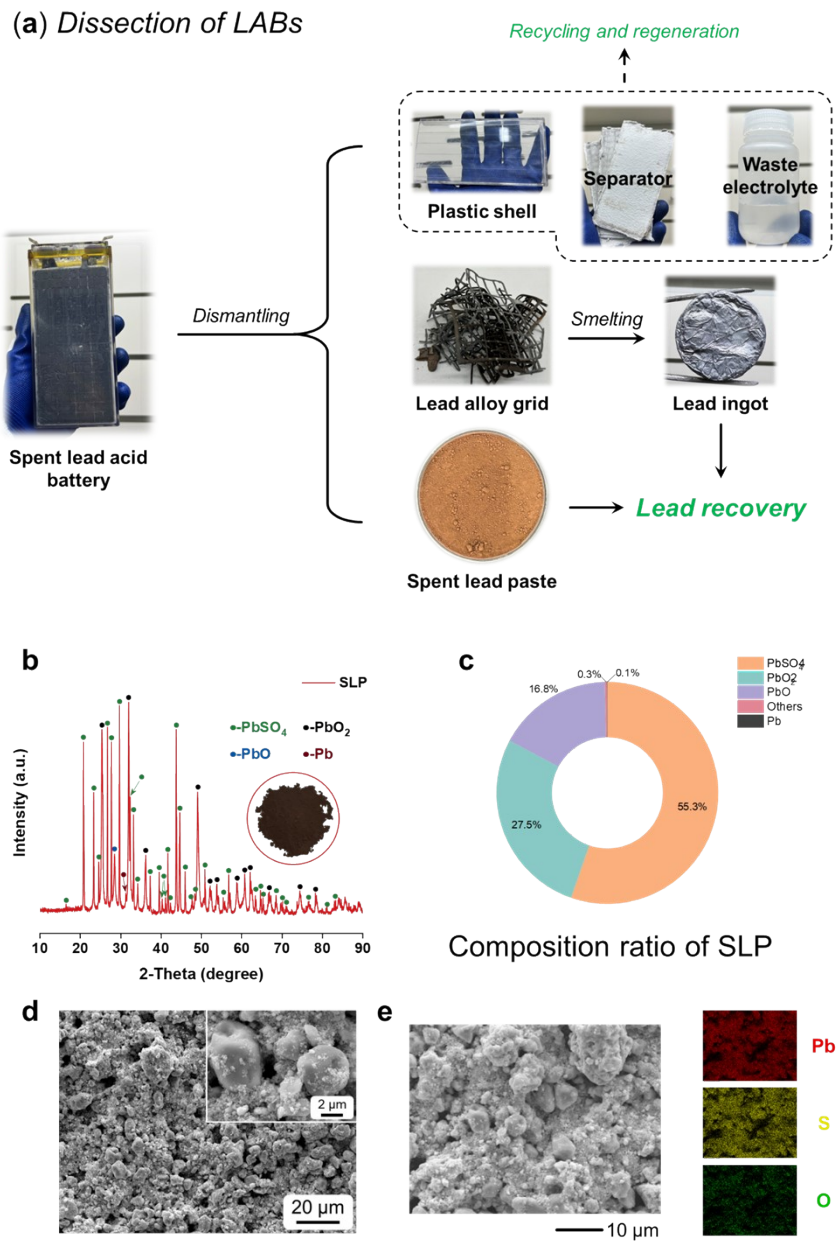

Fig. S3. (a) Schematic of dismantling spent LABs, (b) XRD patterns of spent lead paste (SLP), (c) chemical compositions of SLP, (d) SEM images and (e) the element mappings of SLP.

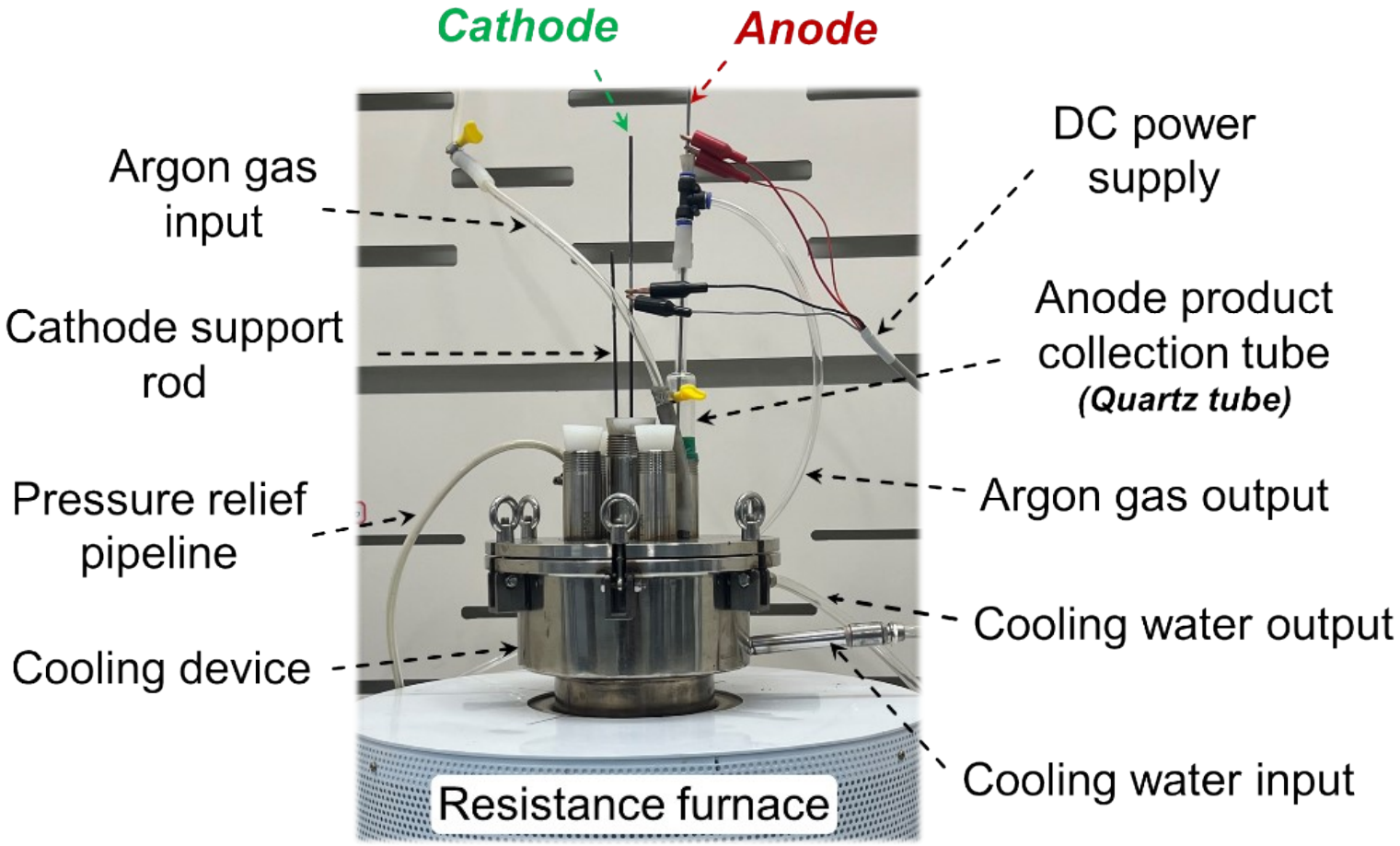

Fig. S4. Optical schematic of the electrolysis reactor.

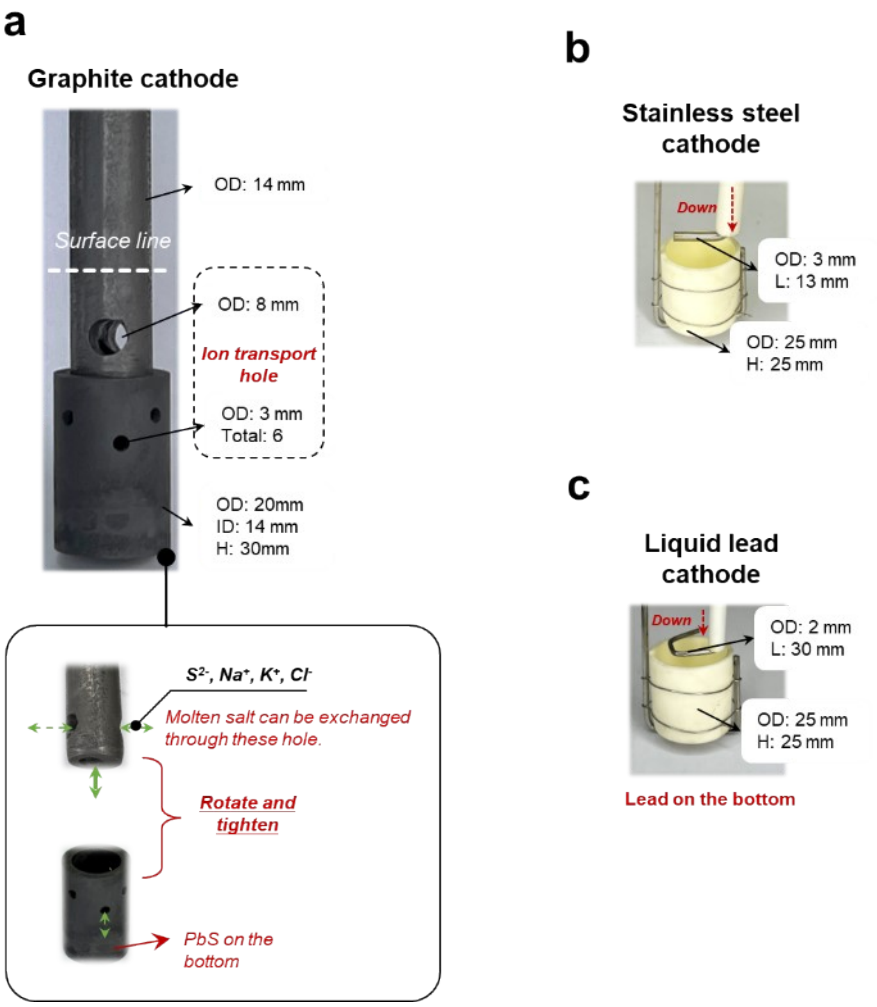

Fig. S5. Optical photos of cathode electrodes: (a)-graphite cathode, (b)-stainless steel cathode, (c)-liquid lead cathode.

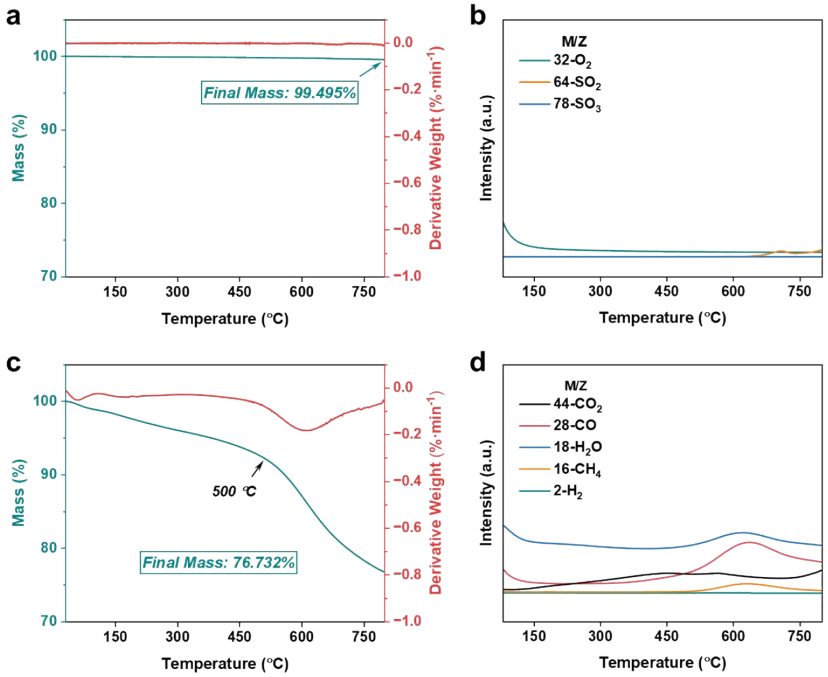

Fig. S6. TG-DTG curves and MS curves of (a & b) $PbSO_4$ and (c & d) charcoal (Heating rate: 20 °C·min^{-1}, Atmosphere: He).

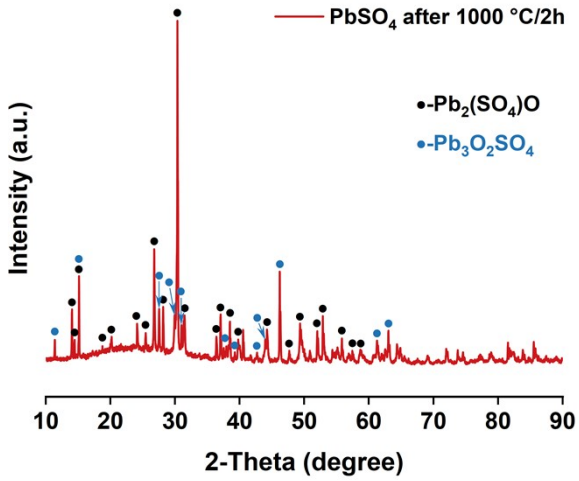

Fig. S7. XRD patterns of $PbSO_4$ roasted at 1000 °C for 2 h (Atmosphere: Ar).

Discussion

$PbSO_4$ remains stable up to 800 °C, exhibiting only a 0.505% mass loss (Fig. S6a). A minimal amount of SO_2 decomposition is observed around 700 °C (Fig. S6b). Subsequently, roasting at 1000 °C for 2 h in an argon atmosphere was conducted, revealing the formation of $Pb_2(SO_4)O$ and $Pb_3O_2SO_4$ phases (Fig. S7), indicating the self-decomposition of $PbSO_4$ upon heating. Furthermore, charcoal contains trace amounts of undecomposed lignin, cellulose, and hemicellulose (Fig. S6c). Gas analysis (Fig. S6d) indicates that the generated gases are primarily H_2O, CO, and CH_4, which can also facilitate the conversion of $PbSO_4$ to PbS.

Molar ratio		
1	**$PbSO_4$**	**1.0000 g**
4	**C**	**0.1584 g**

If the following reaction occurs:

$$\mathbf{PbSO_4 + 2C = PbS + 2CO_2(g)}$$

Then **1.0000 g 0.0792 g 0.7890 g**

So finally

$$\textit{Final mass} = \frac{\text{Final}}{\text{Initial}} = \frac{0.8682\ \text{g}}{1.1584\ \text{g}} \times 100\% = \mathbf{74.946\%}$$

Fig. S8. Final mass analysis of $PbSO_4$-C in TG test.

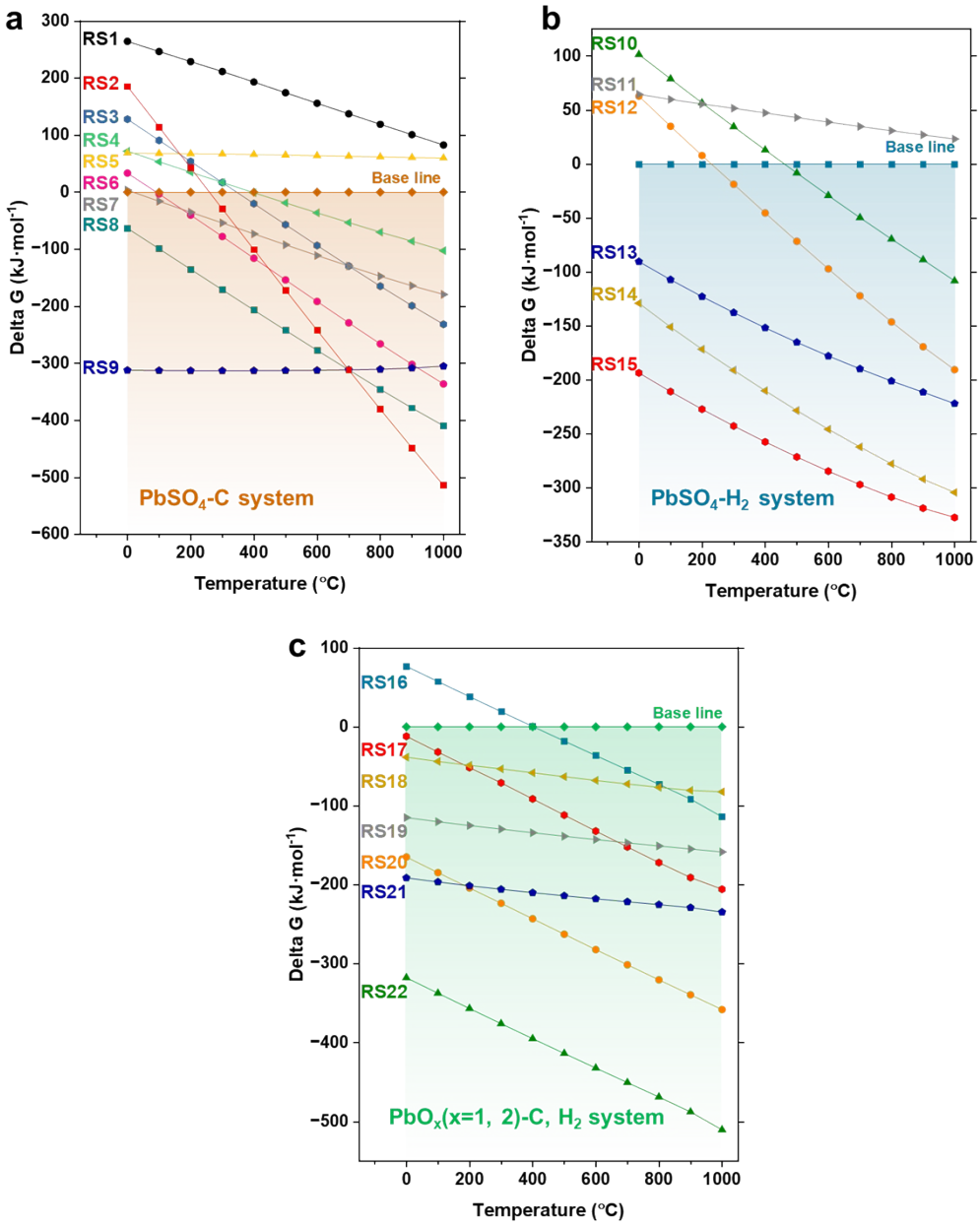

Fig. S9. The standard *Gibbs* free energy as a function of temperature: (a) $PbSO_4$-C system; (b) $PbSO_4$-H_2 system; (c) PbO_x (x = 1, 2)-C, H_2 system (The chemical reaction is shown in **Tab. S1**).

Tab. S1. The corresponding chemical reaction in Fig. S9.

Serial number	Chemical reaction
RS1	$2PbS + C = 2Pb + CS_2(g)$
RS2	$PbSO_4 + 4C = PbS + 4CO(g)$
RS3	$PbSO_4 + C = Pb + SO_2(g) + CO_2(g)$
RS4	$PbSO_4 + CO(g) = PbO + SO_2(g) + CO_2(g)$
RS5	$PbS + CO(g) = Pb + COS(g)$
RS6	$PbSO_4 + 2C = Pb + S + 2CO_2(g)$
RS7	$PbSO_4 + 2CO = Pb + SO_2 + 2CO_2(g)$
RS8	$PbSO_4 + 2C = PbS + 2CO_2(g)$
RS9	$PbSO_4 + 4CO(g) = PbS + 4CO_2(g)$
RS10	$PbSO_4 + H_2(g) = PbO + SO_2(g) + H_2O(g)$
RS11	$PbS + H_2(g) = Pb + 4H_2S(g)$
RS12	$PbSO_4 + 2H_2(g) = Pb + SO_2(g) + 2H_2O(g)$
RS13	$PbSO_4 + 4H_2(g) = PbO + H_2S(g) + 3H_2O(g)$
RS14	$PbSO_4 + 5H_2(g) = Pb + H_2S(g) + 4H_2O(g)$
RS15	$PbSO_4 + 4H_2(g) = PbS + 4H_2O(g)$
RS16	$PbO_2 = PbO + O_2\ (g)$
RS17	$2PbO + C= 2Pb + CO_2(g)$
RS18	$PbO + H_2(g) = Pb + H_2O(g)$
RS19	$1/2PbO_2 + H_2(g) = 1/2Pb + H_2O(g)$
RS20	$PbO_2 + C = Pb + CO_2(g)$
RS21	$PbO_2 + H_2(g) = PbO + H_2O(g)$
RS22	$2PbO_2 + C = 2PbO + CO_2\ (g)$

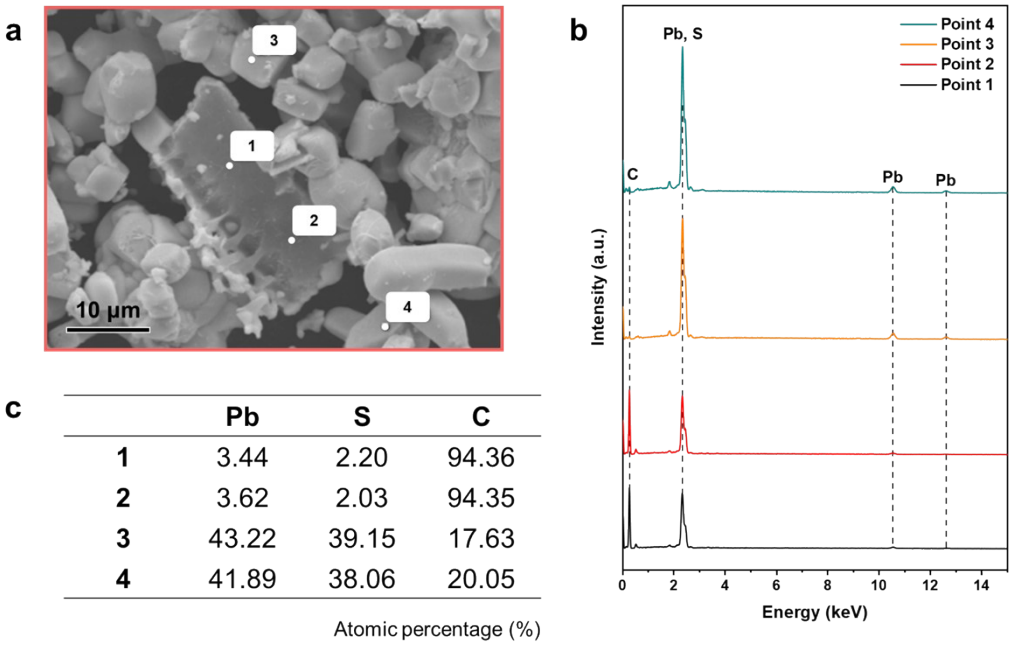

c

	Pb	S	C
1	3.44	2.20	94.36
2	3.62	2.03	94.35
3	43.22	39.15	17.63
4	41.89	38.06	20.05

Atomic percentage (%)

Fig. S10. (a) Samples consistent with Fig. 2e, selected points for EDS spectra, (b) EDS results, and (c) atomic percentage.

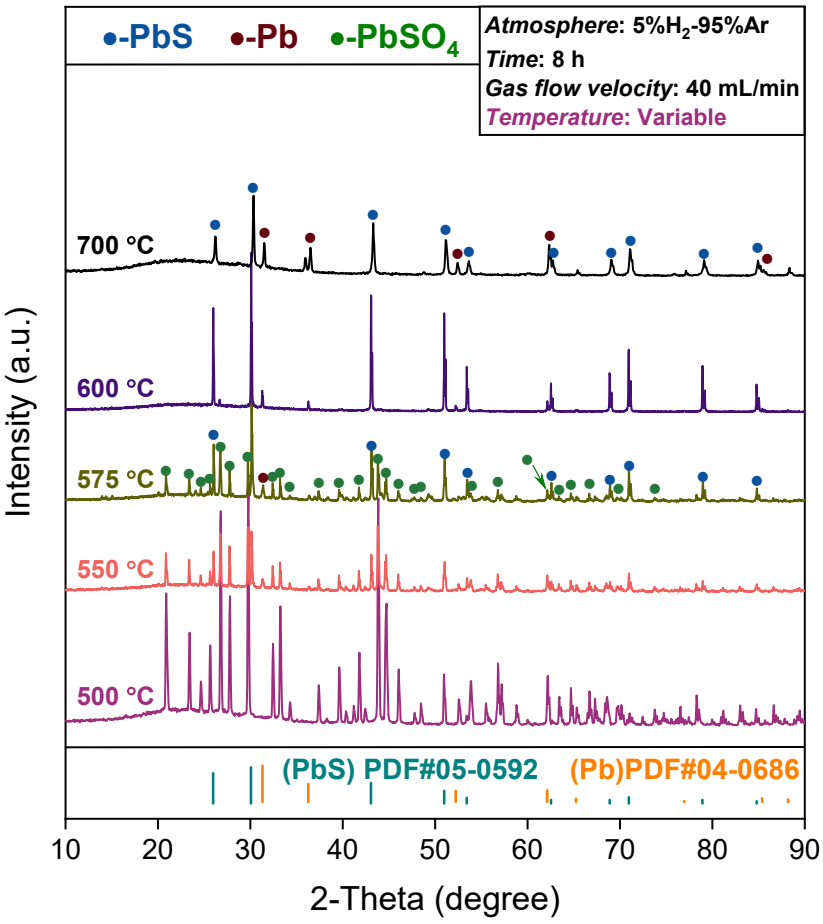

Fig. S11. XRD patterns of hydrogen-thermal reduction of $PbSO_4$ at different temperatures.

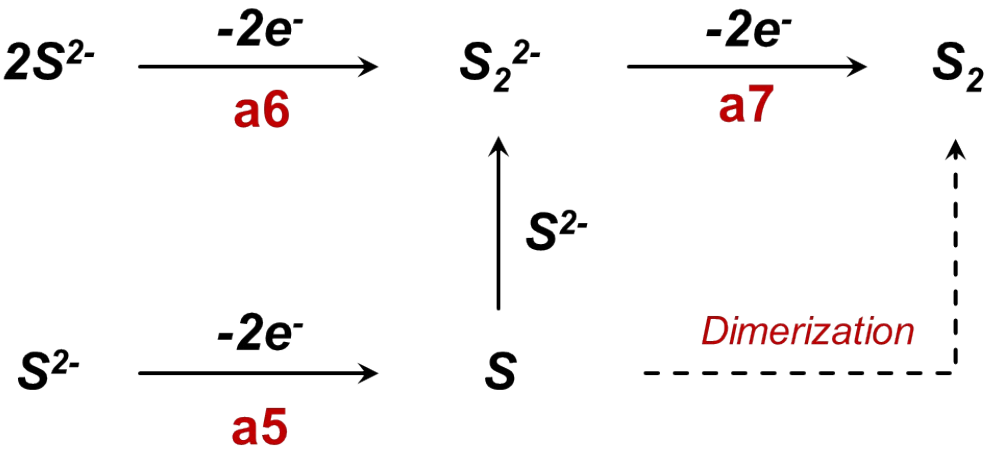

Fig. S12. Evolutionary mechanism of electro-oxidation of S^{2-} to S_2.

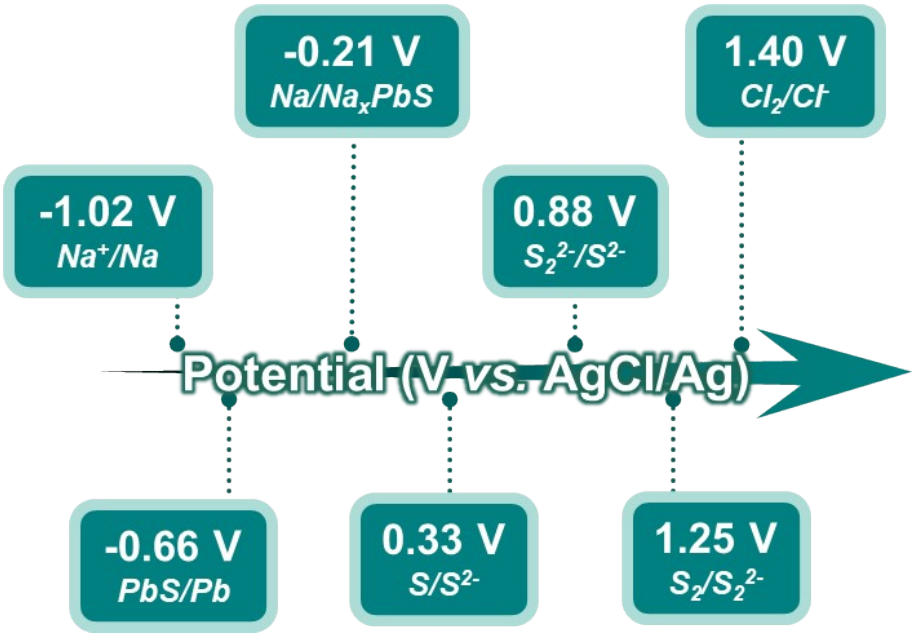

Fig. S13. Sequence of potential electrode reactions.

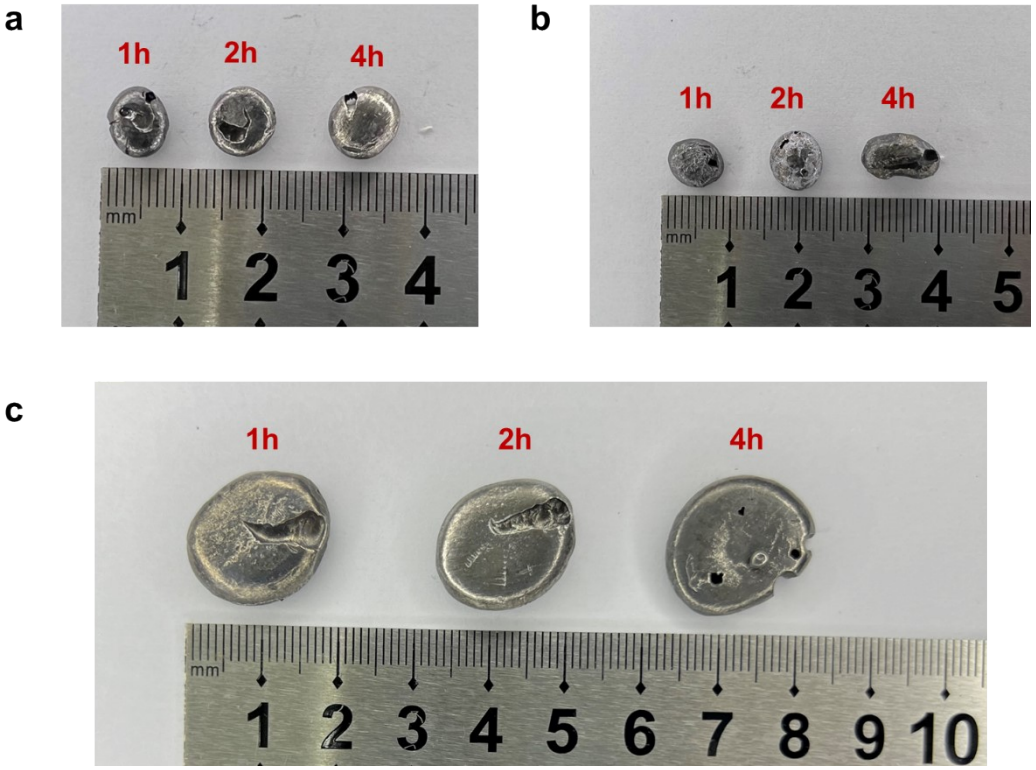

Fig. S14. Optical photos of cathodic products of PbS-electrolysis using different cathodes: (a) graphite cathode, (b) stainless steel cathode, (c) liquid lead cathode.

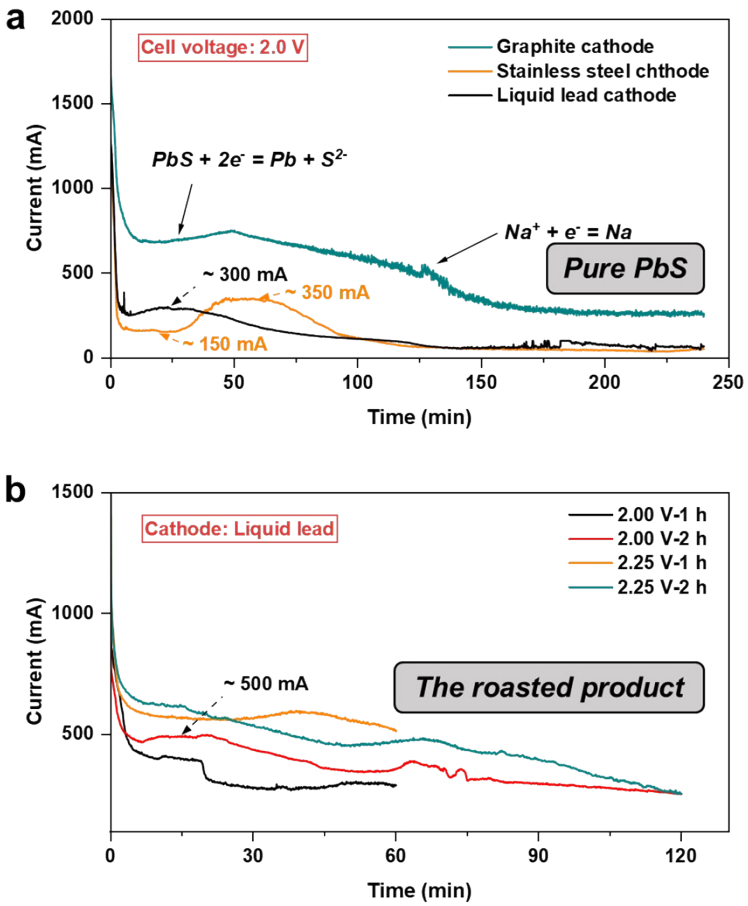

Fig. S15. The current-time plots of electrolysis of (a) pure PbS and (b) the roasted product.

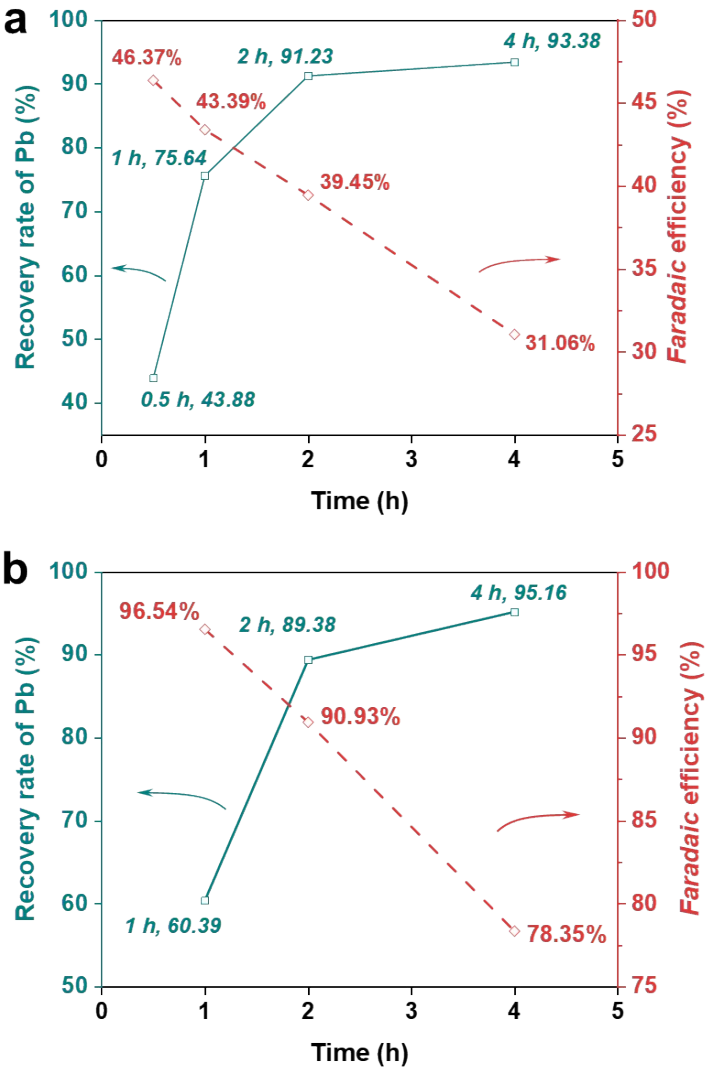

Fig. S16. The *Faradaic* efficiency using (a) graphite cathode and (b) stainless steel cathode.

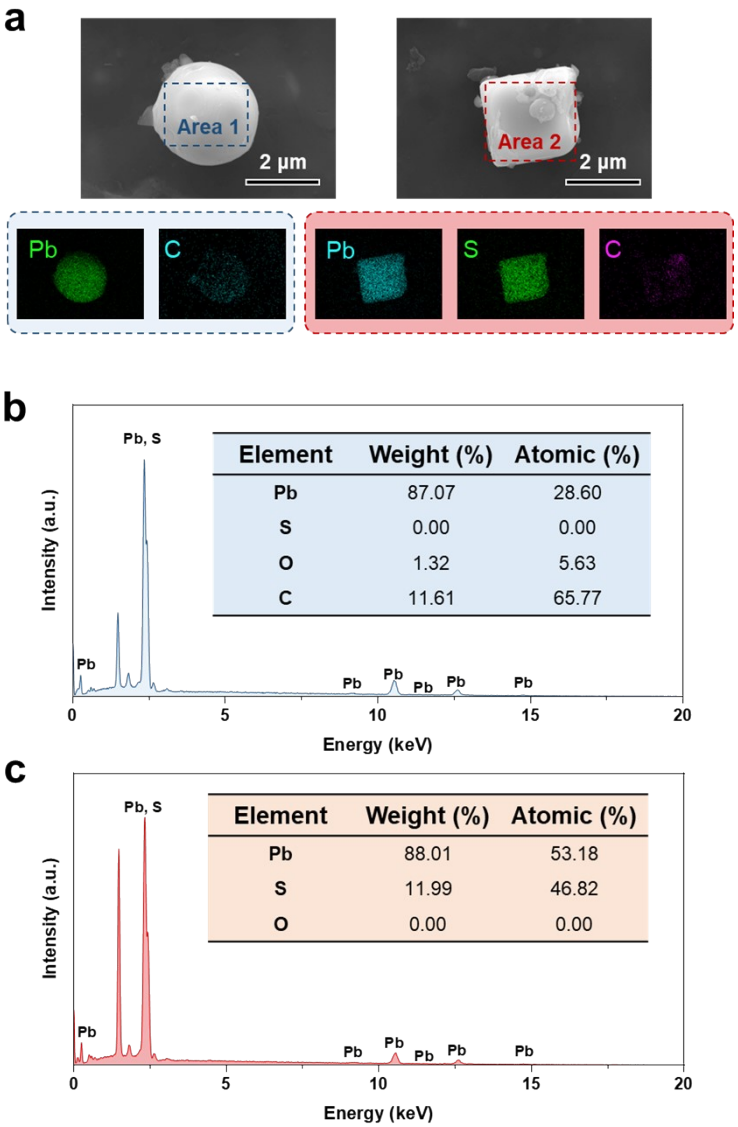

Fig. S17. (a) The element mappings of matter with different morphologies, as well as the EDS and elemental content in (b) Area 1 and (c) Area 2.

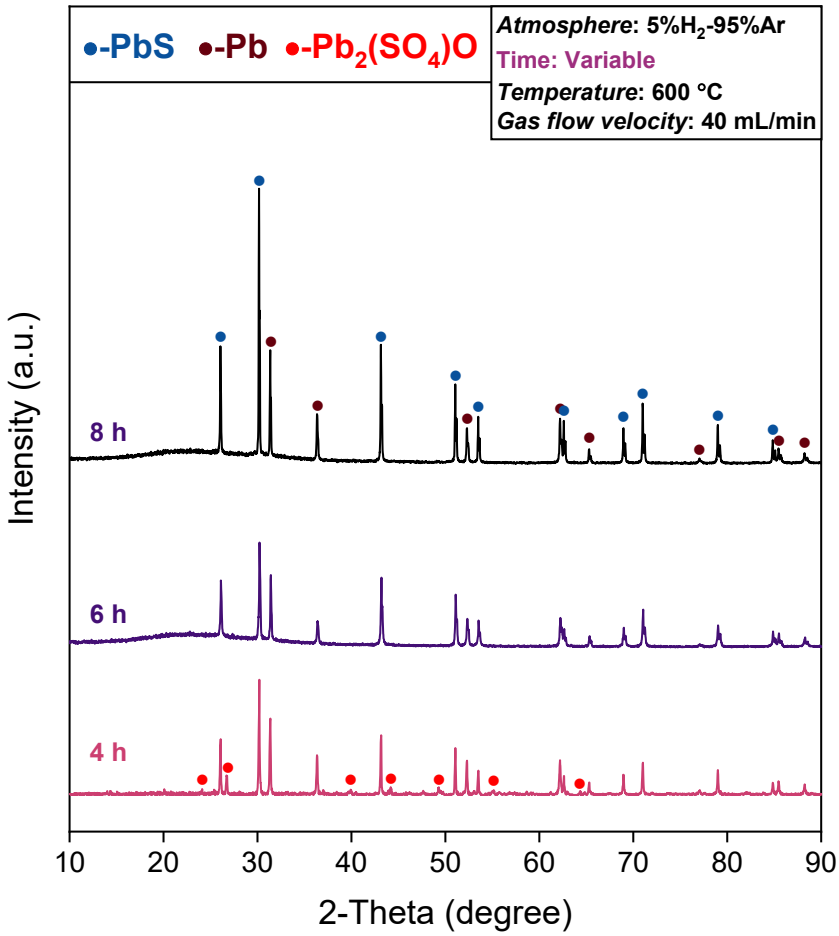

Fig. S18. XRD patterns of hydrogen-thermal reduction of SLP at different times at 600°C.

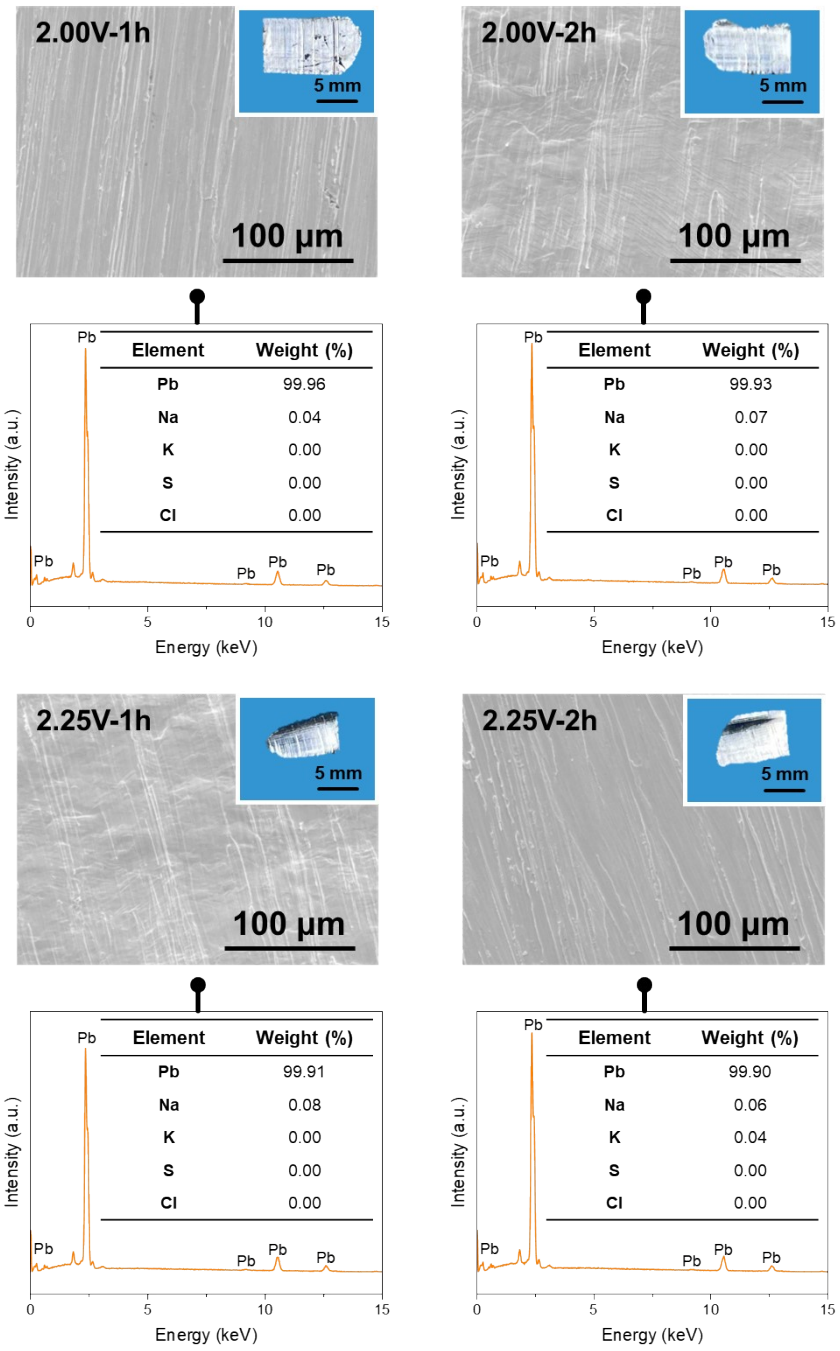

Fig. S19. SEM and EDS of the cross-section of the electrolysis products of roasted product (the inset is the corresponding optical photo).

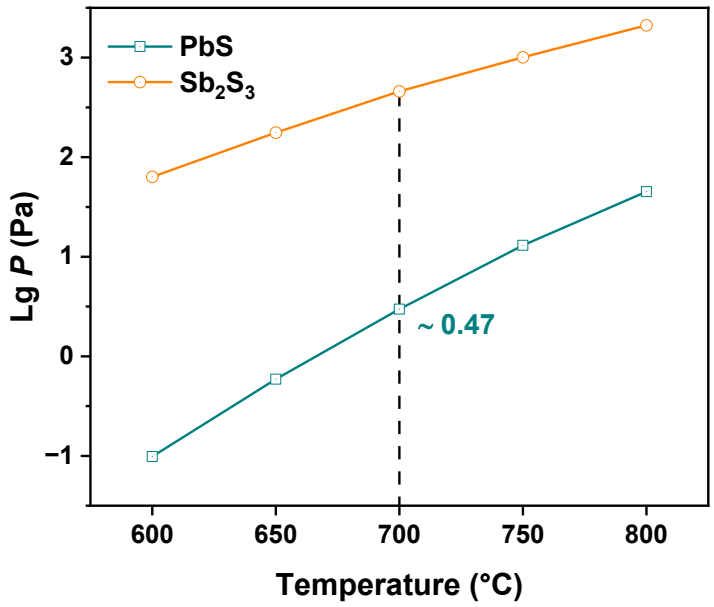

Fig. S20. Relationship curves between the vapor pressure and temperature of PbS and Sb_2S_3.[1]

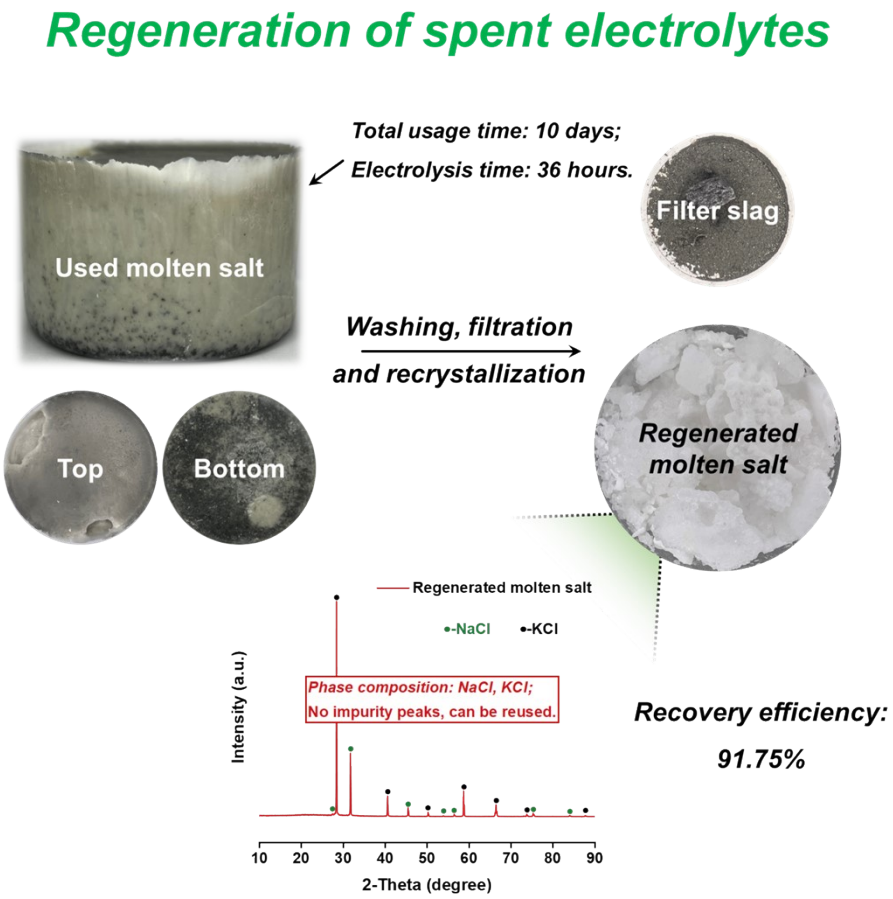

Fig. S21. Schematic of electrolyte regeneration and XRD pattern of regenerated electrolyte.

Tab. S2. Comparison of CO_2 reduction calculations.

	Oxygen-Rich Side-Blown Bath Smelting Process	This work
Energy consumption (kgce·(t-Pb)$^{-1}$)	121.8	39.8
Carbon content (%)	90%	
CO_2 emissions (kg)	401.94	131.34

kgce: kilogram standard coal.

Tab. S3. Recent research progress in SLP recycling.

Methods	Products (containing-Pb)	Pb recovery rate (%)	Flow of sulfate	SO_2 emissions (kg/t-SLP)	Temperature (°C)	*Ref.*
1	Pb	92~95	SO_2	116.83	~1300	—
2	Pb	85~90	Na_2SO_4	—	~700	—
3	Pb	98	Na_2SO_4, SO_2	2.8% (in fume)	1040	Li et al.[2]
4	Pb	93	FeS	~2.34	1150	Li et al.[3]
5	$PbCl_2$	99.7	$CaSO_4$	—	650	Liu et al.[4]
6	Pb	98.13	Na_2SO_4	—	850	Ma et al.[5]
7	PbS	98.37	$CaSO_4$	—	800	Liu et al.[6]
8	$PbCO_3$	99.7	$CaSO_4$	—	80	Chai et al.[7]
9	Pb	95.28	Na_2SO_4	—	90	Chang et al.[8]
10	α-PbO	99.8	$(NH_4)_2SO_4$	—	80	Liu et al.[9]
11	Pb	95.61	$CaSO_4$	—	40	Dai et al.[10]
12	PbO@C	—	Na_2SO_4	—	600	Hu et al.[11]
This work	**Pb**	**97.85**	**S**	**< 5.84**	**700**	—

"—" means nothing here; SO_2 content in fume in red.

Texts:

1-The oxygen-rich side-blown bath smelting process.

2-The sodium carbonate desulfurization process.

3-The low-temperature alkali smelting process.

4-The iron oxide sulfur fixation process.

5-The vacuum-chlorination processes.

6-The hydrometallurgical desulfurization and vacuum thermal reduction.

7-The integrated vacuum chlorinating and hydrothermal process.

8-The enhanced desulfurization method using $(NH_4)_2CO_3$.

9-The hydrometallurgical extraction of lead in the methanesulfonic acid system.

10-The hydrometallurgical extraction of lead in the conjugated solution of ammonium sulfate-ammonia ($(NH_4)_2SO_4$–NH_3).

11-The recovery of high purity lead from SLP *via* direct electrolysis.

12-The synthesis of Nanostructured PbO@C.

***This work*-Thermal reduction-molten salt electrolysis process.**

Calculation of energy consumption for this process (Fig. 7b)

Take Recycling 1 kg SLP as an example:

1. Roasting

1 kg SLP requires 118.8 g charcoal as reductant, of which SLP contains 553 g $PbSO_4$, 275 g PbO_2, and 168 g PbO.

1.1 Input

$\boldsymbol{C_{p,m}}$ (charcoal) = ~0.8 $J \cdot K^{-1} \cdot kg^{-1}$

Q (Charcoal) = $\boldsymbol{C_{p,m}}$ (charcoal) $\cdot m \cdot \Delta t = 0.8 \times 0.1188 \times (650 - 20) = 59.875$ kJ

$\boldsymbol{C_{p,m}}$ (PbSO4) = 104.2 $J \cdot K^{-1} \cdot mol^{-1}$

Q (PbSO4) = $\boldsymbol{C_{p,m}}$ (PbSO4) $\cdot m \cdot (m_{PbSO4})^{-1} \cdot \Delta t = 104.2 \times 553 \times (303.263)^{-1} \times (650 - 20) =$ 119.706 kJ

$\boldsymbol{C_{p,m}}$ (PbO2) = 64.4 $J \cdot K^{-1} \cdot mol^{-1}$

Q (PbO2) = $\boldsymbol{C_{p,m}}$ (PbO2) $\cdot m \cdot (m_{PbO2})^{-1} \cdot \Delta t = 64.4 \times 275 \times (239.199)^{-1} \times (650 - 20) =$ 46.644 kJ

$\boldsymbol{C_{p,m}}$ (PbO) = 49.3 $J \cdot K^{-1} \cdot mol^{-1}$

Q (PbO) = $\boldsymbol{C_{p,m}}$ (PbO) $\cdot m \cdot (m_{PbO})^{-1} \cdot \Delta t = 49.3 \times 168 \times (223.199)^{-1} \times (650 - 20) =$ 23.378 kJ

Q (Input) = 249.603 kJ = **69.334 Wh**

1.2 Furnace temperature maintenance

Taking the treatment of SLP in a $1 \times 1 \times 1$ m^3 volume resistance furnace as an example:

Fill 50% volume of SLP and charcoal mixture, and according to its density of 5.5 $\times 10^3$ $kg \cdot m^{-3}$, it is known that 2750 kg is filled inside.

Its inner surface area is 6 m^2, and the industrial resistance furnace maintains a temperature of 30 kW (5$kW \cdot m^{-2}$, 650 °C).

Baking time of 2 h, electricity consumption of 75 kWh (Thermal efficiency: 80%).

So, P (maintenance) = 27.273 $Wh \cdot kg^{-1}$.

Q (maintenance) = **27.273 Wh**

In addition, the reaction also releases heat during roasting.

2. Electrolysis

2.1 Input of electrolytic power

Each 50 g SLP consumes 2633.6 mAh (scale-up experiment), so 1 kg SLP requires 52.672 Ah. The voltage is 2.2 V, which requires **115.878 Wh** power.

2.2 Temperature maintenance of electrolytic furnace

Similar to the roasting stage, $Q_{(\text{maintenance})}$ = **27.273 Wh**.

Calculations of SO_2 emissions (Fig. 7c)

The possible SO_2 emissions from each process in Table S2 was calculated as 55.3% $PbSO_4$ per ton of SLP (i.e., 553 kg-$PbSO_4$/t-SLP)

1.The oxygen-rich side-blown bath smelting process

All 553 kg $PbSO_4$ is converted to SO_2 in the process, corresponding to 116.83 kg of SO_2 emissions.

2.The sodium carbonate desulfurization process

This process primarily produces Na_2SO_4, and usually the SO_2 emission at this temperature is difficult. However, it's often true that there is nothing that can be done about these sulfur fixers.

3.This work

About 95% of $PbSO_4$ is converted to PbS, with only 5% of $PbSO_4$ producing SO_2 emissions. Therefore, the total SO_2 emissions amount to 5.84 kg.

References

1. Z. Dong, Z. Zhou, H. Xiong, B. Yang and Y. Dai, *Sep. Purif. Technol.*, 2021, **279**, 119776.
2. W. Li, W. Zhang, L. Luo and X. Xie, *Sep. Purif. Technol.*, 2023, **310**, 123156.
3. Y. Li, S. Yang, P. Taskinen, J. He, F. Liao, R. Zhu, Y. Chen, C. Tang, Y. Wang and A. Jokilaakso, *J. Cleaner Prod.*, 2019, **217**, 162-171.
4. K. Liu, J. Yang, S. Liang, H. Hou, Y. Chen, J. Wang, B. Liu, K. Xiao, J. Hu and J. Wang, *Environ. Sci. Technol.*, 2018, **52**, 2235-2241.
5. Y. Ma and K. Qiu, *Waste Manage.*, 2015, **40**, 151-156.
6. K. Liu, S. Liang, J. Wang, H. Hou, J. Yang and J. Hu, *ACS Sustain. Chem. Eng.*, 2018, **6**, 17333-17339.
7. L. Chai, Z. Li, K. Wang, X. Liu, S. Dai, X. Liu, Y. Sun and J. Pan, *Adv. Sci.*, 2023, **10**, 2304863.
8. C. Chang, S. Yang, Y. Li, C. Xiang, H. Wang, S. Liu, T. Luo and Y. Chen, *Sep. Purif. Technol.*, 2023, **306**, 122592.
9. N. Liu, R. A. Senthil, X. Zhang, J. Pan, Y. Sun and X. Liu, *J. Cleaner Prod.*, 2020, **267**, 122107.
10. F. Dai, H. Huang, B. Chen, P. Zhang, Y. He and Z. Guo, *Sep. Purif. Technol.*, 2019, **224**, 237-246.
11. Y. Hu, J. Yang, J. Hu, J. Wang, S. Liang, H. Hou, X. Wu, B. Liu, W. Yu, X. He and R. V. Kumar, *Adv. Funct. Mater.*, 2018, **28**, 1705294.